v1: 3 May 2024

Research Article

Experimental Behavior of Solar Still Using Mixed Oxides Mn-Fe/Silicone Resin Composite as Selective Solar Absorber

Preprinted: 3 April 2024
Peer-approved: 3 May 2024

Qeios, Vol. 6 (2024)
ISSN: 2632-3834

Carlos Eladio Juárez Salinas[1], Reyna Itsamara Ventura Reyes[1], Victor Renteria Tapia[2], Carlos Leopoldo Fernández Rendón[3], Enrique Barrera[4]

1. Department of Processes and Hydraulics, Division of Basic Sciences and Engineering, Universidad Autónoma Metropolitana - Iztapalapa, Mexico; 2. Department of Natural and Exact Sciences, Universidad de Guadalajara, Mexico; 3. Ecotoxicology Laboratory, Department of Hydrobiology, Division of CBS, Universidad Autónoma Metropolitana - Iztapalapa, Mexico; 4. Universidad Autónoma Metropolitana, Mexico

In this research, the optical properties of a black pigment of mixed Mn-Fe oxides synthesized by the precipitation method and dispersed in silicone resin at different concentrations for use as a solar absorber in a two-slope passive solar still were evaluated. The transmittance of different thicknesses of float glass with 0.1% Fe2O3 was also studied for use as a condenser in the construction of the solar still. Regarding the pigments, the absorbance and spectral emittance were evaluated. With the above information, both the absorbent surface and the condensers were optimized to propose the best design of the solar still. The novel hybrid material used as a selective coating in the still, which corresponds to 2.3% Mn-Fe mixed oxides, exhibited a high solar absorbance of 91.82% and a relatively low infrared thermal emission of less than 57.22%, as well as good stability in the corrosive and hot environment of the solar still, in addition to great durability over time and in real operating conditions. The float glass with the highest transmittance corresponds to a thickness of 3 mm and an average transmittance of 82.57%. The built prototype was characterized by obtaining the temperature profiles of the absorber and condensers, thermal efficiency, production, and water quality. The prototype has a thermal efficiency of 29.6%, requiring only energy from the sun for its operation. The water produced by this device becomes an option for human use and consumption in accordance with current official standards, allowing supply in communities that do not have access to drinking water but have access to seawater or waters with high hardness.

Corresponding author: Carlos Eladio Juárez Salinas, juarezsalce@gmail.com

Highlights

- Selective solar absorber based on the mixed oxides Mn-Fe/resin composite
- Design, construction, and characterization of the solar still
- Thermal efficiency analysis of the device
- Distilled water quality analysis

Nomenclature

- H Insolation, [MJ / m^2]
- I Experimental Irradiance; [W / m^2]

 doi.org/10.32388/Z57AR1.2

- $I_s(\lambda)$ Irradiance AM 1.5 G; [W / m^2]
- T Temperature; [K]

Greek letters

- $\alpha(\lambda)$ Spectral absorptance [-]
- α_s Solar absorptance, [-]
- $\varepsilon(\lambda)$ Spectral emittance [-]
- ε_t Thermal emittance; [-]
- η Thermal efficiency; [-]
- $\tau(\lambda)$ Spectral transmittance; [-]
- τ Solar transmittance; [-]

Abbreviations

- EC Escherichia coli
- pH Hydrogen potential
- MPN Most Probable Number
- TDS Total Dissolved Solids, [mg/L]
- BGBLB Brilliant Green Bile Lactose Broth

1. Introduction

Water solar distillation for human consumption is today an attractive alternative since the distilled water produced by the action of solar energy is usually very pure; this technique has received considerable attention from the second half of the 20th century in many regions of the world where seawater is abundant, drinking water is scarce, and solar irradiation is high. Even today, due to its versatility, solar distillation has had growing interest in recent years [1].

Nature itself, based on the water cycle that the oceans follow, is a clear example of how to obtain drinking water by means of solar stills. Being solar distillation the path that the planet's water follows to carry out its cycle, it is reliable to emulate this process to obtain drinking water from seawater or brackish water using these prototypes.

The equipment used to distill water using solar radiation (either passively or actively) is called solar stills, which are useful in hot climates and with a high annual average solar irradiation. The water production depends to a great extent on the dimensioning of the device and the materials used in its manufacture, so improvements are feasible in terms of its efficiency and the total daily water production [2]. Regarding the dimensioning and components, solar stills have many shapes, and the materials used in their manufacture are wide-ranging, but in all, the distillation process is quite similar. Among the main designs, one can find single-slope solar stills, those in the form of a house (also called Australian or two-slope), multiple-effect, those that are greenhouse type, pyramid-shaped [3], those that use solar concentrators [4], those with an inclined tray [5], as well as those that are tubular [6] and in a spherical shape [7], among others. Most use different types of glass or acrylic as a collector cover; in addition, the collecting tubs can be made of glass, fiberglass, acrylic, rubber [8], steel, and there are even some prototypes that are made of ferrocement [9]. In addition, different types of solar radiation-absorbing surfaces can be mentioned in terms of their structure, which can be conventional, with fins, or corrugated absorber surfaces, among others [10]. Insulating materials are of many types as well, and among them, we can mention glass wool, cardboard, and polyurethane, among others [11].

As noted above, various technological materials with specific optical and thermal properties are required in the fabrication of these photothermal systems. In particular, the selective absorber coatings deposited on metallic substrates play an important role in the

efficiency of the photothermal conversion of solar radiation. Solar absorber surfaces ideally should exhibit high thermal and chemical stability, high absorptance (>0.95) in the wavelength range from 0.3 up to 2.5 μm, and low emittance (<0.10) in the infrared region (2.5-25 μm) at the operating temperature of the device. In order to achieve these requirements, a variety of selective absorber coatings and paints have been produced [12]. Specifically, the metal-oxide/dielectric composites have shown good thermal performance at low cost, and in particular, when the dielectric is an organic medium such as silicone resin. Generally, resins have low electrical and thermal conductivity, although these properties are notably improved by using absorber pigments for solar thermal applications. The particle size, concentration, thickness of the coatings, and dispersion of the pigment have an important effect on the solar optical properties [13]. One of the most popular pigments is Fe_2O_3:Mn, which is composed of crystalline hematite and bixbyite phases, exhibiting high solar absorptance in the 0.75 to 0.94 range and low emittance in the range of 0.03 to 0.07 [13]. Similarly, high transmittance in the solar spectrum of the condenser covers is required to favor the greenhouse effect in the solar still.

Improving the configuration of conventional solar stills to increase productivity has always been the concern of engineers and researchers in the field of solar energy and related topics. The time-consuming and expensive manufacturing processes of solar stills motivate researchers to perform mathematical and computational fluid dynamics (CFD) simulations of solar stills to estimate productivity [14]. The literature review reveals that many other studies can be carried out in the future on the CFD simulation of solar stills in which various techniques such as the use of nanotechnology, best reflectors, storage materials, fans, and fins have been considered to improve the efficiency of solar desalination systems [15].

Referring to the current problems in Mexico, there are several places far from the cities that lack drinking water but have hard or brackish water both superficially, underground, and maritime that could be used through purification methods that are economically viable and consistent with the environment. According to the National Water Program 2014-2018 [16], almost nine million people lack drinking water (five million are in rural areas), and 11 million lack sewerage (7.8 million in rural areas), making it essential to address the problem of water shortage. It becomes essential to use solar energy seriously, when appropriate, to desalinate seawater in places where unique hydrological, geographical, and physical conditions exist with competitive costs.

2. Materials and Methods

The synthesis of iron-manganese oxides used as solar selective coating was carried out by the co-precipitation method. They were prepared by using the precursors $FeCl_3{\cdot}6H_2O$ (97%) and $MnCl_2{\cdot}4H_2O$ (97 %) purchased from Sigma-Aldrich. Both salts were dissolved in deionized water and mixed in the appropriate amount to obtain the desired molar ratio of Fe / Mn= 1/3. The stoichiometry ratio between Fe and Mn strongly influences the optical properties of the composites. The mixture was precipitated using a concentrated solution of sodium hydroxide NH_4OH (28%, Sigma-Aldrich) under stirring at a temperature of 60 °C. Throughout the precipitation process, the pH was maintained above 10. The resulting precipitate was washed several times with distilled water and calcined at 800 °C for 1 h. Once the oxides had been obtained, they were mixed with commercial acetic silicone from the Sista trademark at different concentrations in the range from 2.3-13% wt to determine the one with the highest solar absorptance and low emittance. This silicone is transparent with a density of 1.02 g/ml, extrusion of 370 g/ml, elongation of 480%, and a curing time of 24 h. Similarly, in order to optimize the transmittance of the condenser cover made of glass, different thicknesses of this material were considered. Afterward, the optimization of the better materials for the construction of the solar still, the metal-oxide/resin hybrid material was applied in a thin film on the metal substrate of the distiller by means of a stiff bristle brush, leaving an absorbing layer in the order of 300 μm thick.

For the characterization of the condenser (float glass with 0.1% of Fe_2O_3), its transmittance in the solar region (300 to 2500 nm) was evaluated with a Varian 5E UV-Vis-NIR spectrophotometer, and an integration was made over the solar region to obtain the average values of the transmittance of each condenser candidate. The expression that allows the average transmittance to be derived from the spectrum transmittance is [17]:

$$\tau = \frac{\int I_s(\lambda)\tau(\lambda)d\lambda}{\int I_s(\lambda)d\lambda} \quad (1)$$

Where λ is the wavelength, $\tau(\lambda)$ is the spectral transmittance, and $I_s(\lambda)$ is the normal solar irradiance, corresponding to the AM 1.5 G.

The crystal structure of the solar absorber samples was obtained through X-ray diffraction patterns on a Bruker D8 Advance diffractometer with Cu-Kα radiation, operating in Bragg-Brentano geometry. Patterns were obtained in an interval of 15° to 108° in 2θ with a step of 0.020414° and 76.8 s per point.

The spectral reflectance of black pigments in the range of 300 to 2500 nm was obtained from a Varian 5E UV-Vis-NIR spectrophotometer using an integrating sphere. Once spectral reflectance $\rho(\lambda)$ had been obtained, spectral absorptance could be found through the formula [18] $\alpha(\lambda) = 1 - \rho(\lambda)$, considering that the system is in thermal equilibrium. Average absorptance is obtained through expression [17][18]:

$$\alpha_s = \frac{\int I_s(\lambda)\alpha(\lambda)d\lambda}{\int I_s(\lambda)d\lambda} \quad (2)$$

Where λ is the wavelength, $\alpha(\lambda)$is the spectral absorptance, and $I_s(\lambda)$ is the normal solar irradiance, ideally corresponding to the AM 1.5 G.

The spectral reflectance $\rho(\lambda)$ of the samples in the range of 2500-25000 nm was obtained using a Nicolet iS50 FT-IR spectrophotometer. The spectral emittance is obtained from the expression [18] $\varepsilon(\lambda) = 1 - \rho(\lambda)$

The average emittance is derived from the expression [17][18]:

$$\varepsilon_t = \frac{\int E(\lambda,T)\varepsilon(\lambda)d\lambda}{\int E(\lambda,T)d\lambda} \quad (3)$$

Where $E(\lambda,T)$ represents the Planck blackbody emission spectrum at 120 °C and whose expression is:

$$E(\lambda,T) = \frac{c_1}{\lambda^5\left(e^{\frac{c_2}{\lambda T}} - 1\right)} \quad (4)$$

Being $c_1 = 3.7405x10^{20}\ Wnm^4m^{-2}$ and $c_2 = 1.43879x10^7\ nm\ K$.

In the case of surface profilometry, a Stylus Bruker Dektak XT profilometer was used to sweep an area of dimensions 1 mm x 1 mm to determine the roughness of the samples and to obtain a three-dimensional image of each sample.

The efficiency of the still [19] is the relationship between the useful heat $\int_o^t qdt$ throughout the day and the total insolation H received:

$$\eta = \frac{\int_o^t q\,dt}{H} \bullet 100 \quad (5)$$

Where H, the daily insolation, is given by

$$H = \int_o^t Idt \quad (6)$$

and where I is the experimentally observed irradiance.

Regarding the water quality study, the input water to the module and the output water were compared with respect to the permissible limits, characterizing the odor, flavor, pH,

hardness, total dissolved solids, salinity, total coliforms, and fecal coliforms.

To measure the pH of the inlet and outlet water, a high-precision Webat portable pH meter was used; hardness was determined using a HACH 5-B hardness test kit; total dissolved solids were measured using a Hanna Instruments HI98302 total dissolved solids meter with a high range that can measure up to 10.00 g/L; finally, salinity was evaluated using an Atago ATC-S/Mill-E refractometer.

3. Results and Discussion

In order to optimize the performance of the solar still, different variables related to the crystal structure, the optical properties of the materials used for the construction of the solar still, as well as their morphology, were studied. The thickness of the collector glass cover, the influence of the concentration of mixed Mn-Fe oxides dispersed in the silicone resin on the absorption and emittance, and the morphology of the samples were considered.

3.1. Crystal Structure

Fig. 1 shows the diffraction patterns of the mixed oxides of Mn-Fe; these coincide with the reflection maxima reported in the ICDD-PDF 04-016-1434, ICDD-PDF 04-024-5003, and ICDD-PDF 01-074-9811 cards and correspond to the $MnFeO_3$, $Mn_{0.2}Fe_{2.8}O_4$, and $Fe_{0.84}Mn_{1.16}O_3$, all these oxides with cubic structure.

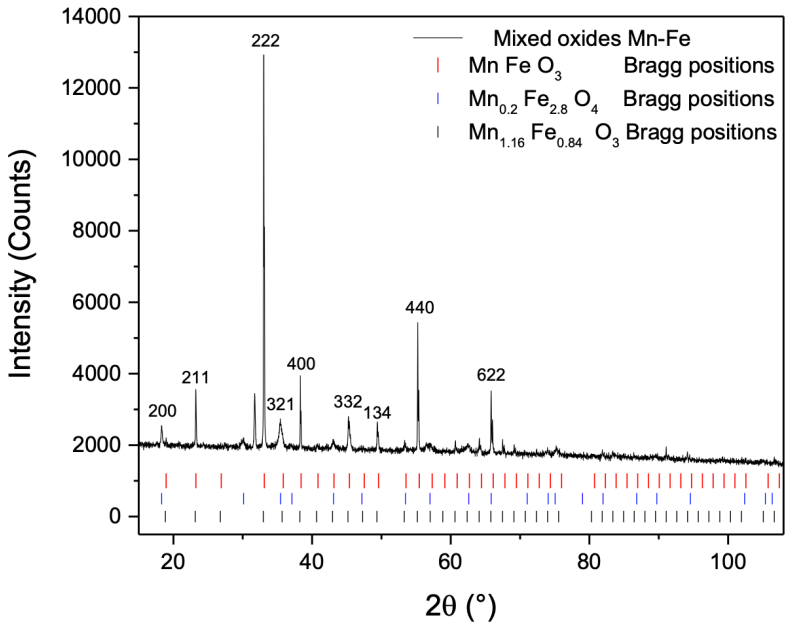

Fig. 1. Diffraction pattern of Mn-Fe oxides. The pattern shows a mixed composition of phases and the Bragg indices corresponding to the predominant phase $MnFeO_3$.

3.2. Optical properties

The transparent cover of different thicknesses with 0.1% Fe_2O_3 in the range of 300 to 2500 nm has been characterized (Fig. 2), obtaining an average weighted transmittance of 82.59% for the 3 mm thick glass cover. Table 1 shows the average transmittance for different thicknesses of float glass.

doi.org/10.32388/Z57AR1.2

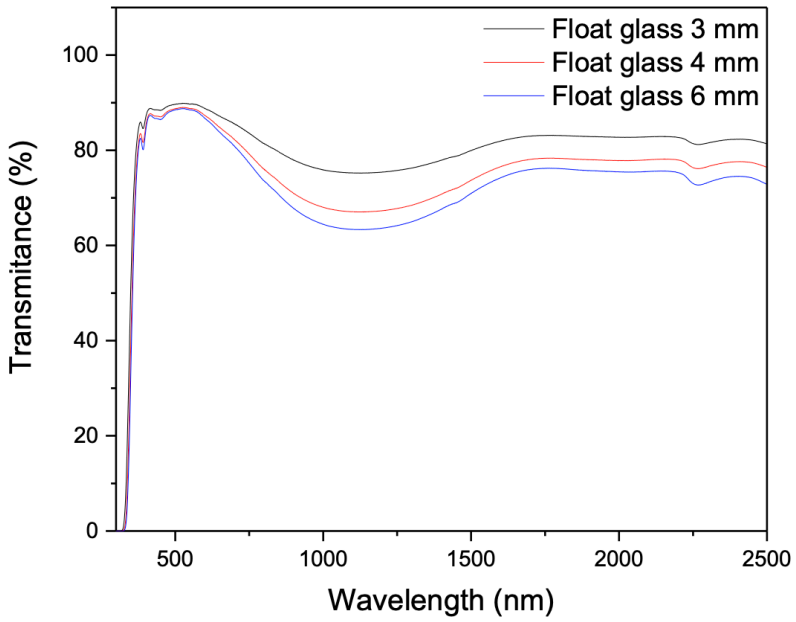

Fig. 2. Spectral transmittance of 0.1% Fe2O3 float glass with different thicknesses. The condenser with the highest transmittance corresponds to the one that has a thickness of 3 mm.

Condenser	τ (%)
3 mm	82.59
4 mm	78.43
6 mm	76.58

Table 1. Average transmittance values for different thicknesses of float glass with 0.1% Fe_2O_3.

On the other hand, the highest average solar absorption of 91.82% was achieved in the range of 300 to 2500 nm for Mn-Fe pigment oxides at a concentration of 2.3 % by weight (Fig. 3). The spectral emittance for different concentrations of Mn-Fe oxides is shown in Figure 4; the estimation of the emittance values for the MnFeO3/resin compound was 57.52%, also at a concentration of 2.3%.

doi.org/10.32388/Z57AR1.2

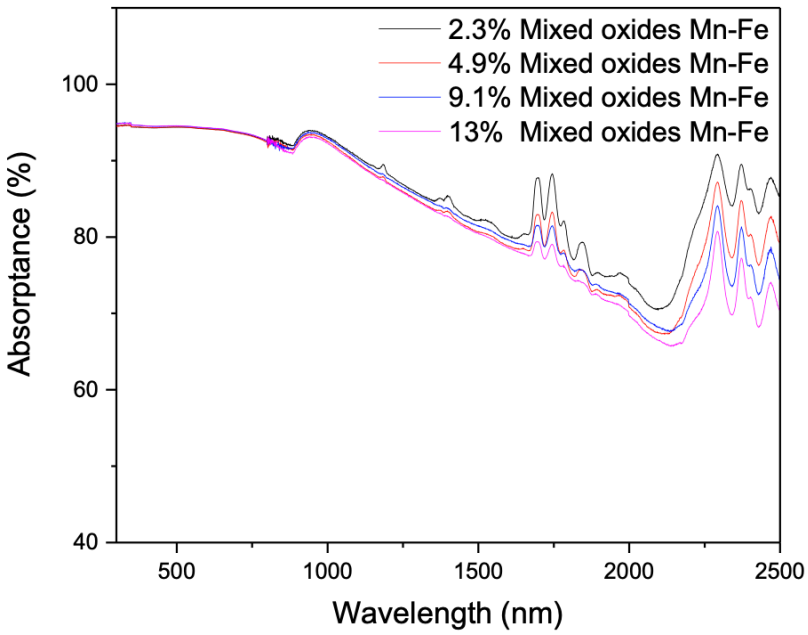

Fig. 3. Spectral solar absorptance for the powders of mixed oxides Mn-Fe in adhesive silicone at different concentrations.

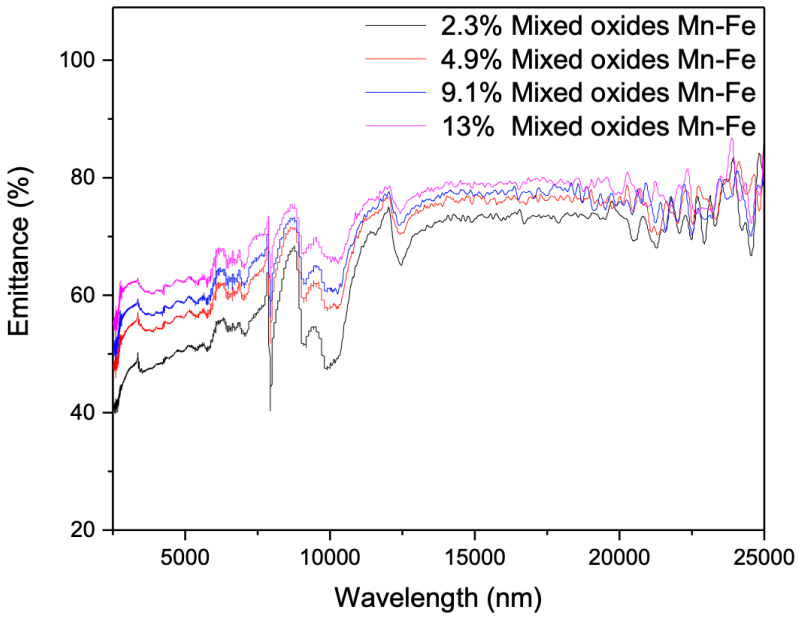

Fig. 4. Emittance for the powders of mixed oxides Mn-Fe in adhesive silicone at different concentrations.

Table 2 summarizes the values of absorption, emittance, and selectivity of each of the samples. As can be seen, the 2.3% sample exhibits the best optical behavior since it has

doi.org/10.32388/Z57AR1.2

the highest absorption and the lowest emittance.

Sample	α (%)	ε (%)
2.3% Mixed oxides Mn-Fe	91.82	57.22
4.9% Mixed oxides Mn-Fe	91.29	62.98
9.1% Mixed oxides Mn-Fe	91.45	65.15
13% Mixed oxides Mn-Fe	91.12	68.39

Table 2. Values of the absorptance and emittance of each sample.

3.3. Morphological properties

Through surface profilometry studies with the Stylus Bruker Dektak XT profilometer, three-dimensional images of the absorbent films have been obtained in areas of 1 mm^2 for each of the samples, and their roughness has been obtained. Fig. 5 is an example image of the surface, obtaining roughness values of 4312.558 nm.

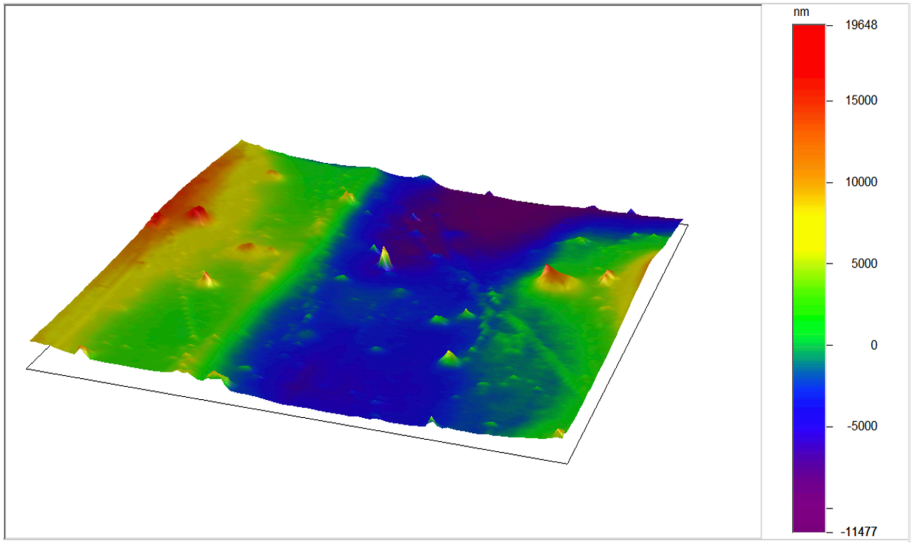

Fig. 5. Surface profilometry of Mn-Fe oxides in silicone in an area of 1 mm^2. The roughness is 4312.558 nm.

3.4. Construction of the solar still

After various tests on sizing and materials, an Australian-type still was built (Fig. 6) with 1 m^2 of solar radiation collection area, and the condenser covers are made of clear glass. The transparent glass cover is 3 mm thick and has better transmittance (82.59%) compared with glass of greater thickness, favoring the heat flow to the environment from the condensers. The box (base, walls, and gutters) is made of fiberglass due to its low thermal conductivity of 0.04 W/m-K and is manufactured in one piece to minimize liquid losses due to leaks. The absorber was made with a mixture of silicone and iron-manganese oxides at 2.3% wt due to its mechanical stability and easy production, having a solar absorptance of 91.82% and an average emittance of 57.22%. The inclination of the roofs is 16°, and the height of the water mirror is between 1 cm and 4 cm thick to ensure

doi.org/10.32388/Z57AR1.2

the fast evaporation desired in the technique. Fig. 6 shows a scheme of the solar distillation experimental prototype.

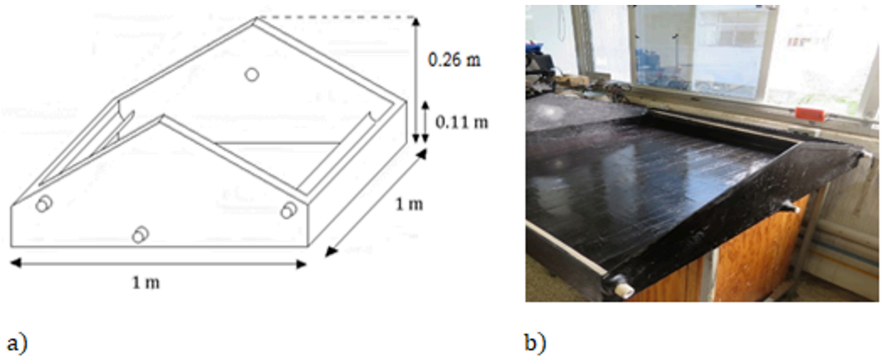

Fig. 6. a) Schematic diagram of the two-slope fiberglass still. b) Fe_2O_3:Mn/silicon hybrid solar absorber picture, applied to the bottom of the solar still.

3.5. Efficiency

The calculation of thermal efficiency is carried out by dividing the useful heat throughout the day by the total insolation H received (see equations 5 and 6), so it is necessary to quantify the water production per hour, the latent evaporative heat as a function of the temperature, as well as the radiation received from the sun at each hour of the day. Figure 7 shows the temperature of the solar absorber, the east and west condensers (Figure a), as well as the irradiance throughout the day (Figure b) for some days in March.

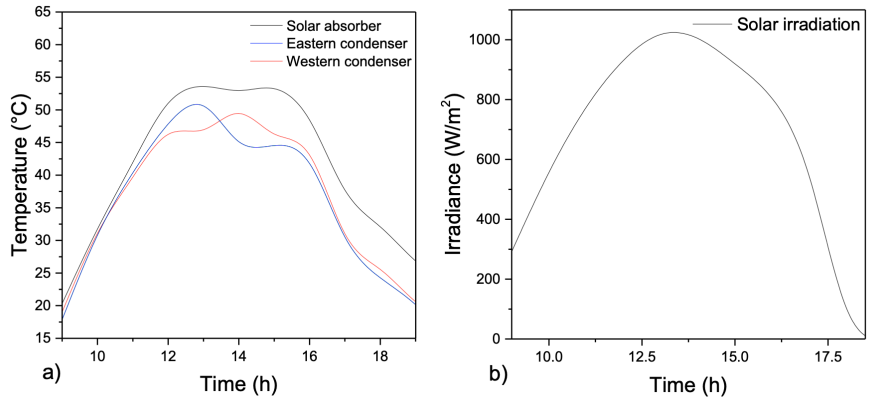

Fig. 7. a) Temperature values in the solar absorber and condensers for each hour. b) Solar irradiance for each hour.

Figure 8 shows the hourly distilled water production (Figure a) and the cumulative distilled water production (Figure b) from 9:00 to 19:00.

doi.org/10.32388/Z57AR1.2

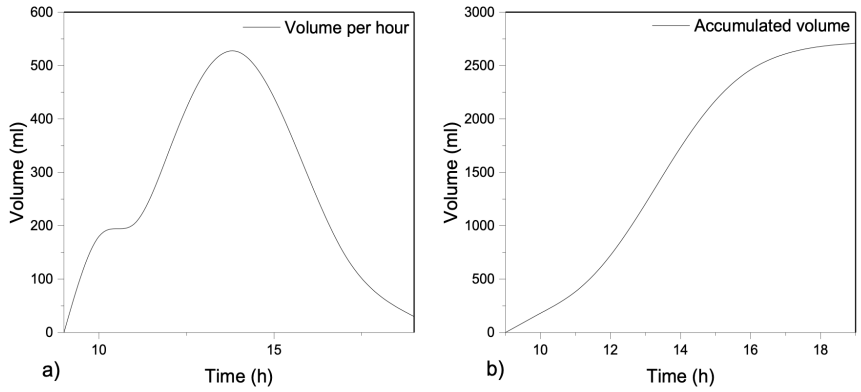

Fig. 8. a) Production of distilled water for every hour. (b) Production of accumulated distilled water for each hour.

Taking into account the above, calculations have been made for different days; the data used range from the month of October to the month of March. Table 3, by way of example, shows the values of water production, useful heat, daily insolation, and efficiency of the device for some days in March. For these days, a maximum efficiency value of 27% was obtained. At this point, it is necessary to highlight the fact that the characterization of the device was carried out during the seasons of the year with less daily irradiation. Therefore, water production and efficiency will be higher during the summer.

Distilled water production (kg)	Useful heat per m^2(MJ/m^2)	Daily insolation H (MJ/m^2)	Thermal Efficiency η (%)
2.8	6.8	23.0	29.6

Table 3. Useful heat, insolation, and efficiency values.

3.6. Water quality

The study consisted of comparing the inlet water to the module and the outlet water with respect to the permissible limits according to what is stipulated in the official Mexican standards [20][21]. Two types of studies were carried out: the first consisted of taking tap water and the corresponding distilled water at the exit; the second consisted of taking simulated seawater (water with 3.5% sodium chloride) and the corresponding distilled water from the prototype output.

The tests carried out for the study consisted of comparing the inlet water to the module and the outlet water with respect to the 48 parameters that NOM-127-SSA1-1994 considers to determine the quality of a water sample. Despite this, and due to the large number of studies that must be carried out to determine the quality conclusively, only the most representative parameters were selected to determine water quality through our research group, which are: smell, taste, pH, hardness, total dissolved solids, salinity, total coliforms, and fecal coliforms.

For the presence of coliforms, water samples were inoculated, in different dilutions, in a series of test tubes with a Durham bell; these tubes contained lactose as a culture medium. The tubes were examined at 24 and 48 hours of incubation at 37°C. Each of those that presented turbidity with gas production was reseeded in a more selective confirmatory

medium. In the case of total coliforms, the confirmatory study was made in tubes with BGBLB (Brilliant Green Bile Lactose Broth), incubated at 37°C for 48 hours. For fecal coliforms, the study was done in tubes with Escherichia coli broth (EC broth) incubated at 44.5°C for 24 hours. Using statistical tables, the most probable number (MPN) of total and fecal coliforms in 100 cm^3 of sample was calculated, from the numbers of the tubes that gave positive confirmatory results [21].

Table 4 shows the results obtained in the water quality study for input samples of tap water and simulated seawater and compared with the distilled output water for each of them, as well as the maximum values accepted by NOM-127-SSA1-1994.

Parameter	Tap water (entry)	Tap water distilled (exit)	Salt water (entry)	Water distilled (exit)	Permissible limit by NOM 127 SSA
Taste	_____	Pleasurable	_____	Pleasurable	Pleasant (not objectionable from a biological or chemical point of view).
Salinity (g/L)	3	3	35	3	_____
Smell	_____	Pleasurable	_____	Pleasurable	Pleasant (not objectionable from a biological or chemical point of view).
Total Coliforms (MPN / 100ml)	23	Not detectable	180	Not detectable	Absence or undetectable
Fecal Coliforms (MPN / 100ml)	Not detectable	Not detectable	27	Not detectable	Absence or undetectable
pH	8.6	7.8	7.9	7.3	6.5-8.5
TDS (mg/L)	861	13	9370	11	1000
Water Hardness (mg/L)	450	20	550	20	500

Table 4. Parameter data measured to determine the quality of distilled water.

As presented in Table 4, each of the parameters is within the norm. Preliminarily, and with regard to these studies, the water is appropriate for human consumption, since not only are the imposed limits not exceeded, but also each parameter is well below what is permissible; however, it must be emphasized that in order to have a convincing characterization, it is necessary to evaluate each parameter of the update of NOM-127-SSA1-1994.

4. Conclusions

This research has made it possible to obtain a sustainable, low-cost, easy-to-maintain prototype with a thermal efficiency of 29.6%. This efficiency was achieved with the solar absorber of 2.3% Mn-Fe oxides, with an absorptance of 91.82% and an emittance of 57.22%, and with an average condenser transmittance of 82.59%. In terms of daily water production, the device produces an average of 2.8 L of water. Regarding the quality of distilled water, for the two water samples studied, corresponding to tap water and

simulated seawater, the measured parameters are below the values required by the Mexican standard NOM-127-SSA1-1994. In the bacteriological studies, neither total coliforms nor fecal coliforms were detected for both distilled water from tap water and for distilled water from simulated seawater. The high quality of water distilled by means of solar stills suggests that it should be considered a priority due to its great energy and environmental relevance. It is of great importance to continue the study of passive solar distillation from the perspective of improving thermal efficiency, sizing, and exergetic studies that allow increasing daily water production.

Statements and Declarations

Data Availability

The raw data supporting the conclusions of this article will be made available by the authors upon reasonable request. Inquiries can be directed to the corresponding author.

Author Contributions

Barrera C, E: Conceptualization, Methodology, Software, Supervision, and Project administration. **Renteria T. V**: Experimental Methodology. **Juarez S, C**: Investigation, Formal analysis, Visualization, and Writing. **Fernández R, C**: Resources and Investigation. **Ventura R, R**: Writing and Revision.

Acknowledgments

The support provided by the National Council of Science and Technology (CONACYT, Mexico) through project No. 60781 and the PEMA, belonging to the national register of postgraduate courses CONACYT (agreement 003893), is appreciated. Víctor Rentería is grateful to CONACYT.

References

1. ^*Zhang Y, Sivakumar M, Yang S, Enever K, Ramezanianpour M (2018). "Application of solar energy in water treatment processes: A review." Desalination. **428**:116–145. doi:10.1016/j.desal.2017.11.020.*
2. ^*Sarkar MNI, Sifat AI, Reza SS, Sadique MS (2017). "A review of optimum parameter values of a passive solar still and a design for southern Bangladesh." Renewables: Wind, Water, and Solar. **4**(1):1–13. doi:10.1186/s40807-017-0038-8.*
3. ^*Nayi KH, Modi KV (2018). "Pyramid solar still: A comprehensive review." Renewable and Sustainable Energy Reviews. **81**:136–148. doi:10.1016/j.rser.2017.07.004.*
4. ^*Altarawneh I, Batiha M, Rawadieh S, Alnaief M, Tarawneh M (2020). "Solar desalination under concentrated solar flux and reduced pressure conditions." Solar Energy. **206**:983–996. doi:10.1016/j.solener.2020.06.058.*
5. ^*Murugavel KK, Anburaj P, Hanson RS, Elango T (2013). "Progresses in inclined type solar stills." Renewable and Sustainable Energy Reviews. **20**:364–377. doi:10.1016/j.rser.2012.10.047.*
6. ^*Thalib MM, Manokar AM, Essa FA, Vasimalai N, Sathyamurthy R, Garcia Marquez FP (2020). "Comparative Study of Tubular Solar Stills with Phase Change Material and Nano-Enhanced Phase Change Material." Energies. **13**(15):3989. doi:10.3390/en13153989.*
7. ^*Modi KV, Nayi KH, Sharma SS (2020). "Influence of water mass on the performance of spherical basin solar still integrated with parabolic reflector." Groundwater for Sustainable Development. **10**:100299. doi:10.1016/j.gsd.2019.100299.*
8. ^*Kabeel AE, El-Agouz SA (2011). "Review of researches and developments on solar stills." Desalination. **276**(1-3):1–12. doi:10.1016/j.desal.2011.03.042.*
9. ^*Muñoz F, Barrera E, Ruiz A, Martínez EM, Chargoy N (2020). "Long-term experimental theoretical study on several single-basin solar stills." Desalination. **476**:114241. doi:10.1016/j.de*

sal.2019.114241.

10. ^Arunkumar T, Wang J, Rufuss DDW, Denkenberger D, Kabeel AE (2020). "Sensible desaltin g: Investigation of sensible thermal storage materials in solar stills." Journal of Energy Stor age. **32**:101824. doi:10.1016/j.est.2020.101824.
11. ^Selvaraj K, Natarajan A (2018). "Factors influencing the performance and productivity of s olar stills - A review." Desalination. **435**:181–187. doi:10.1016/j.desal.2017.09.031.
12. ^Wijewardane S, Goswami DY (2012). "A review on surface control of thermal radiation by paints and coatings for new energy applications." Renewable and Sustainable Energy Revi ews. **16**(4):1863–1873. doi:10.1016/j.rser.2012.01.046.
13. a, bHernández-Pérez CD, Barrera-Calva E, González F, Rentería Tapia V (2021). "Ultrasonic spray pyrolysis technique to generate a solar absorber coating of Mn-doped α-Fe_2O_3." Ren ewable Energy and Environmental Sustainability. **6**:3. doi:10.1051/rees/2021003.
14. ^Karimi Estahbanati MR, Ahsan A, Feilizadeh M, Jafarpur K, Ashrafmansouri SS, Feilizade h M (2016). "Theoretical and experimental investigation on internal reflectors in a single-sl ope solar still." Applied Energy. **165**:537–547. doi:10.1016/j.apenergy.2015.12.047.
15. ^Rajaseenivasan T, Prakash R, Vijayakumar K, Srithar K (2017). "Mathematical and experi mental investigation on the influence of basin height variation and stirring of water by sol ar PV panels in solar still." Desalination. **415**:67–75. doi:10.1016/j.desal.2017.04.010.
16. ^Comisión Nacional del Agua (2014). "National Water Program 2014-2018." http://www.co nagua.gob.mx/conagua07/contenido/documentos/PNH2014-2018.pdf.
17. a, b, cDuffie JA, Beckman WA, Blair N (2020). Solar engineering of thermal processes, photo voltaics and wind. John Wiley & Sons.
18. a, b, c, dDe Maio D, D'Alessandro C, Caldarelli A, De Luca D, Di Gennaro E, Russo R, Musto M (2021). "A selective solar absorber for unconcentrated solar thermal panels." Energies. **14**(4): 900. doi:10.3390/en14040900.
19. ^Malik MAS, Tiwari GN, Kumar A, Sodha MS (1982). Solar distillation: a practical study of a wide range of stills and their optimum design, construction, and performance. New York, EUA: Pergamon Press.
20. ^NORMA Oficial Mexicana NOM-127-SSA1-1994 (1994). "Environmental health, Water for human use and consumption, Permissible quality limits and treatments to which water m ust be subjected for its potabilization."
21. a, bNORMA Oficial Mexicana NOM-210-SSA1-2014 (2014). "Products and services. Microbiol ogical test methods, Determination of indicator microorganisms. Determination of pathog enic microorganisms."

Declarations

Funding: The support provided by the National Council of Science and Technology (CONACYT, Mexico) through project No. 60781 and the PEMA, belonging to the national register of postgraduate courses CONACYT (agreement 003893) is appreciated
Potential competing interests: No potential competing interests to declare.